ORIGINAL RESEARCH

Adipose-Derived Exosomes Exert Proatherogenic Effects by Regulating Macrophage Foam Cell Formation and Polarization

Zulong Xie, MD, PhD;* Xuedong Wang, MD;* Xinxin Liu, MD, PhD; Huaan Du, MD, PhD; Changbin Sun, MD; Xin Shao, MD; Jiangtian Tian, MD, PhD; Xia Gu, MD; Hailong Wang, MD; Jinwei Tian, MD, PhD; Bo Yu, MD, PhD

***Background*—**Obesity is causally associated with atherosclerosis, and adipose tissue (AT)–derived exosomes may be implicated in the metabolic complications of obesity. However, the precise role of AT-exosomes in atherogenesis remains unclear. We herein aimed to assess the effect of AT-exosomes on macrophage foam cell formation and polarization and subsequent atherosclerosis development.

***Methods and Results*—**Four types of exosomes isolated from the supernatants of ex vivo subcutaneous AT and visceral AT (VAT) explants that were derived from wild-type mice and high-fat diet (HFD)–induced obese mice were effectively taken up by RAW264.7 macrophages. Both treatment with wild-type VAT exosomes and HFD-VAT exosomes, but not subcutaneous AT exosomes, markedly facilitated macrophage foam cell generation through the downregulation of ATP-binding cassette transporter (ABCA1 and ABCG1)–mediated cholesterol efflux. Decreased expression of liver X receptor-α was also observed. Among the 4 types of exosomes, only HFD-VAT exosomes significantly induced M1 phenotype transition and proinflammatory cytokine (tumor necrosis factor α and interleukin 6) secretion in RAW264.7 macrophages, which was accompanied by increased phosphorylation of NF-κB-p65 but not the cellular expression of NF-κB-p65 or IκB-α. Furthermore, systematic intravenous injection of HFD-VAT exosomes profoundly exacerbated atherosclerosis in hyperlipidemic apolipoprotein E–deficient mice, as indicated by the M1 marker (CD16/32 and inducible nitric oxide synthase)–positive areas and the Oil Red O/Sudan IV–stained area, without affecting the plasma lipid profile and body weight.

***Conclusions*—**This study demonstrated a proatherosclerotic role for HFD-VAT exosomes, which is exerted by regulating macrophage foam cell formation and polarization, indicating a novel link between AT and atherosclerosis in the context of obesity.
(*J Am Heart Assoc*. 2018;7:e007442. DOI: 10.1161/JAHA.117.007442.)

Key Words: adipose tissue • atherosclerosis • exosome • macrophage • obesity

Obesity is a well-established risk factor for atherosclerosis.[1] Individuals with excess deposition of adipose tissue (AT) exhibit increased coronary plaque vulnerability and coronary plaque progression as well as high cardiovascular event rates.[2–4] In recent decades, AT is being recognized as an active endocrine organ that secretes hundreds of bioactive substances, such as adipokines and proinflammatory cytokines.[5] The endocrine function of fat tissue provides crucial clues to the mechanisms linking obese AT with atherosclerosis. It was reported that adipokines and cytokines from accumulated visceral fat play an important role in atherogenesis by influencing lipid and glucose metabolism and by directly affecting vascular function in the context of obesity.[6,7] However, the mode of communication between AT and atherosclerosis remains to be further explored.

Exosomes are small biological vesicles (30–100 nm in diameter) that are actively and constitutively secreted from a wide range of cell types by the fusion of multivesicular endosomes with the plasma membrane.[8] Exosomes enclose diverse cytosolic components and may act as mediators of communication between cells of various tissues and vascular disease.[9] Adipocyte-derived microvesicles (including exosomes) have been shown to deliver adipocyte-dominant transcripts (mRNAs and microRNAs) into macrophages and

From the Department of Cardiology, The Second Affiliated Hospital of Chongqing Medical University, Chongqing, China (Z.X., H.D.); Departments of Cardiology (X.W., X.L., C.S., J.T., X.G., H.W., J.T., B.Y.), and Urology (X.S.), The Second Affiliated Hospital of Harbin Medical University, Harbin, China; Department of Cardiology, Heilongjiang Provincial Hospital, Harbin, China (X.G.).

*Dr Xie and Dr Wang contributed equally to this work.

Correspondence to: Bo Yu, MD, PhD, or Jinwei Tian, MD, PhD, Department of Cardiology, The Second Affiliated Hospital of Harbin Medical University; 246 Xuefu Road, Nangang District, Harbin 150086, China. E-mails: yubodr@163.com, tianjinweidr2009@163.com

Received August 21, 2017; accepted January 30, 2018.

Clinical Perspective

What Is New?

- Visceral adipose tissue from obese mice use exosome to modulate macrophage foam cell formation and M1 macrophage polarization, thereby promoting the development of atherosclerosis in vivo.

What Are the Clinical Implications?

- Exosome serves as a novel mechanistic link between visceral obesity and atherosclerosis, thus it may be a promising therapeutic target for the attenuation of atherosclerotic vascular disease in the growing obese population.

promote AT macrophage activation.[10,11] A recent study confirmed that AT substantially contributes to circulating exosomal miRNA content in both humans and mice[12] and, therefore, might be a major source of circulating exosomes. Whether adipose-derived exosomes have an impact on the initiation and progression of atherosclerosis in an endocrine manner remains to be determined.

Macrophage foam cell formation is a central hallmark in the pathogenesis of atherosclerosis.[13–15] Cellular cholesterol levels depend on a balance among the uptake, efflux, and endogenous synthesis of cholesterol. Uncontrolled uptake of oxidized low-density lipoprotein (oxLDL) via scavenger receptors, including CD36 and scavenger receptor A, promotes the generation of foam cells.[16] Conversely, the impairment of cholesterol efflux, which is mainly mediated by the ATP-binding cassette (ABC) transporters ABCA1 and ABCG1, also leads to an excessive deposition of cholesterol in the cytoplasm of macrophages.[17] In addition, macrophages polarize toward a classic M1 or an alternative M2 phenotype in response to various stimuli in the local microenvironment.[18] M1 macrophages increase and sustain the ongoing inflammatory response by producing proinflammatory mediators.[19] Persistent induction of M1 macrophages promotes an inflammatory state and causes tissue injury, which are associated with atherosclerosis progression and plaque rupture.[20,21] In contrast, M2 macrophages have an antiatherogenic effect through inflammation resolution, tissue repair, and efferocytosis.[19,22] Overall, macrophage foam cell formation and polarization are both fundamental contributors to the development and progression of atherosclerotic plaques.

In the present study, we evaluated the impact of exosomes released by subcutaneous AT (SAT) and visceral AT (VAT) explants isolated from obese and lean mice on macrophage foam cell generation and polarization, compared the effect of these AT-secreted exosomes under physiological or pathologically obese conditions, and investigated the related molecular mechanisms involved in macrophages. Moreover, we examined whether the systemic administration of AT-derived exosomes (AT-exosomes) accelerated atherosclerosis development in vivo.

Methods

The authors declare that all supporting data are available within the article. The analytic methods and study materials are available from the corresponding author upon reasonable request.

Experimental Animals

Eight-week-old C57BL/6J male mice, obtained from the laboratory animal center of The Second Affiliated Hospital of Harbin Medical University, were fed either a high-fat diet (HFD) with 60% of total calories from fat (D12492; HFK Bioscience) or a standard chow diet containing 4% fat (D12450B; HFK Bioscience) for 16 weeks. Body weight was measured biweekly. At the end of the diet intervention, the HFD-induced obese mice had a body weight >30% higher than that of the control mice. All mice were euthanized, and VAT and SAT were separately collected.

Weaned apolipoprotein E–deficient (ApoE−/−) mice on a C57BL/6J background were purchased from HFK Bioscience. After a 2-week period of acclimatization, ApoE−/− mice were fed an HFD (D12079B; HFK Bioscience) to induce atherosclerosis and were administered exosomes derived from the VAT (VAT exosomes) or SAT (SAT exosomes) of HFD-induced obese mice or wild-type (WT) mice through tail intravenous injections (9 mice per group, 30 μg per mouse) every 4 days. The control group was injected with equal volumes of PBS. The mice were euthanized after 6 weeks. Among them, 6 in each group were applied to the histopathological assays of the isolated aortic arteries. The plasma was obtained following blood collection through centrifugation at 815 g for 15 minutes and frozen in −80°C for subsequent lipid profile assays. The aortas of the remaining mice were collected and lysates were then subjected to Western blotting to assess the in vivo expression of target proteins.

All animal experiments were performed according to the *US National Institutes of Health Guidelines for the Care and Use of Experimental Animals* and were approved by the ethics review board of Harbin Medical University.

Isolation of AT-Exosomes and Transmission Electron Microscopy

Isolated ATs were cut into small pieces with appropriate dimensions (not more than 4×4 mm) after rinsing in sterilized

PBS followed by incubation in DMEM-F12 supplemented with 50 mg/mL streptomycin and 50 IU/mL penicillin for 12 hours. Culture supernatants were centrifuged for 30 minutes at 2000 g, and filtered through 0.22-μm membrane filters to remove cells and debris and then used for exosome isolation. Exosome pellets were then acquired from the purified supernatants using total exosome isolation reagent (from cell culture media) (4478359; Life Technologies) according to the manufacturer's instructions. Finally, the exosomes were resuspended in serum-free RPMI1640 medium. The total protein content of exosomes was quantified using the bicinchoninc acid method, and the level of exosomes was presented as micrograms of total protein in exosomes. The ultrastructural morphology of various types of exosomes (HFD-SAT exosomes, WT-SAT exosomes, HFD-VAT exosomes, and WT-VAT exosomes) was identified using a JEM 1220 electron microscope based on negative staining as previously described.[23]

In Vitro Exosome Uptake Assays

Exosomes were labeled using PKH67 Fluorescent Cell Linker kits (Sigma-Aldrich) according to the manufacturer's instructions and then washed 3 times in PBS buffer and resuspended in RPMI1640. The supernatants of the last PBS washing were recognized as exosome-depleted fraction. Next, 10 μg/mL labeled exosomes were incubated with RAW264.7 macrophages for 12 hours. 4',6-Diamidino-2-phenylindole and phalloidin were separately used to stain the cell nucleus and cytoskeleton. Macrophages were incubated with the exosome-depleted fraction to eliminate the possibility of fluorescence leakage. After incubation, macrophages were washed, fixed, and examined using a fluorescence microscope (DMI4000B; Leica).

Intracellular Cholesterol Assessment

RAW264.7 macrophages were pretreated with different groups of AT-exosomes (10 μg/mL) or PBS for 12 hours in RPMI1640 culture medium containing 0.5% BSA followed by coincubation with or without 50 μg/mL oxLDL (YB-002; Yiyuanbiotech) for 24 hours. Then, the cells were washed 3 times with PBS and fixed with 4% paraformaldehyde for 20 minutes at room temperature. After sufficient washing in PBS, cells were washed briefly with 60% isopropanol 3 times and stained with filtered Oil Red O solution at room temperature for 30 minutes. The nucleus was stained with hematoxylin. Stained cells were observed with phase-contrast microscopy (IX71; Olympus).

After incubation with oxLDL, intracellular lipids in macrophages were extracted with a hexane/isopropanol (3:2) mixture and then dissolved with isopropanol containing 10% Triton X-100. Cellular protein was extracted with NaOH (0.2 mol/L). Free cholesterol and total cholesterol were measured with cholesterol detection kits (Applygen) according to the manufacturer's instructions and normalized to cellular protein levels, which were determined with the bicinchoninc acid method. Cholesterol ester content was obtained by subtracting free cholesterol from total cholesterol.

Cholesterol Uptake Assessment

Cholesterol uptake was assessed via immunofluorescence and flow cytometry. Macrophages were pretreated with or without 10 μg/mL exosomes for 12 hours and incubated with 10 μg/mL Dil-oxLDL (YB-0010; Yiyuanbiotech) for 4 hours at 37°C. Fluorescence images were captured using a fluorescence microscope. The mean fluorescence intensity was measured by flow cytometry.

NBD-Labeled Cholesterol Efflux Assay

RAW264.7 macrophages were equilibrated with 1 μg/mL nitrobenzoxadiazole (NBD)-cholesterol (13221; Cayman) in serum-free RPMI1640 medium containing 0.2% BSA for 24 hours. The NBD–cholesterol-loaded cells were rinsed and treated with 10 μg/mL exosomes or PBS for 2 hours. Then, 15 μg/mL apolipoprotein A1 (ApoA1) (A0722; Sigma-Aldrich) or 50 μg/mL high-density lipoprotein (HDL) (YB-003; Yiyuanbiotech) was added into the culture medium to induce cholesterol efflux. NBD-labeled cholesterol efflux was measured at an excitation of 470 nm and emission of 530 nm using a Microplate Reader (Tecan Infinite M200; LabX). ApoA1 or HDL-mediated cholesterol efflux was expressed as the percentage of fluorescence in the medium to the total amount of fluorescence.

Macrophage Phenotype Analysis by Flow Cytometry

Raw264.7 macrophages were treated with 10 μg/mL exosomes or an equal volume of PBS (negative control) in serum-free RPMI1640 for 24 hours. Positive control groups for M1 and M2 polarization were incubated with lipopolysaccharide (500 ng/mL) or interleukin (IL)-4 (20 ng/mL) under equal conditions. Then, the cells were harvested and stained with specific antibodies for 30 minutes at 4°C in the dark. After washing with PBS, the stained cells were analyzed by flow cytometry (FACSCanto II; Becton-Dickinson) to determine the M1 and M2 macrophage phenotype. PE-antimouse CD80, FITC-antimouse CD206, APC-antimouse F4/80, and corresponding isotype controls (104707, 141703, 123115; Biolegend)

were used in this procedure. Data analysis was performed with FlowJo software (FlowJo LLC).

Western Blotting

Western blotting analysis was performed to determine the protein expression levels of exosomal markers, molecules related to cholesterol trafficking, and macrophage polarization. To detect the expression of proteins associated with macrophage foam cell formation, Raw264.7 cells were pretreated with or without 10 μg/mL exosomes in serum-free medium for 24 hours before incubation with or without 50 μg/mL oxLDL for an additional 6 hours. The induction of macrophage polarization was performed as described for flow cytometry analysis. Total lysates were extracted and separated on SDS-PAGE (8–12%) before transfer to nitrocellulose transfer membranes (PALL). After blocking with 5% nonfat milk, membranes were incubated with specific primary antibodies against TSG101 (ab125011; Abcam), Alix (ab186429; Abcam), CD9 (ab92716; Abcam), heat shock protein cognate 70 (ab2788; Abcam), scavenger receptor A (ab183725; Abcam), CD36 (ab133625; Abcam), low-density lipoprotein receptor (ab52818; Abcam), ABCA1 (NB400-105; Novus Biologicals), ABCG1 (sc-11150; Santa Cruz), liver X receptor α (LXR-α) (ab176323; Abcam), peroxisome proliferator-activated receptor γ (PPAR-γ) (WL01800; Wanleibio), phosphor-NF-κB-p65 (3033; Cell Signaling Technology), NF-κB-p65 (8242; Cell Signaling Technology), IκB-α (8242; Cell Signaling Technology), and β-actin (Zhongshan Golden Bridge Biotechnology). The membranes were then incubated with horseradish peroxidase–conjugated secondary antibodies. β-Actin was used as the internal control. The protein bands were visualized using an enhanced chemiluminescence kit (Beyotime) and quantified by densitometry analysis with ImageJ software (National Institutes of Health).

Quantitative Real-Time Polymerase Chain Reaction

Total RNA was extracted from cells using Trizol reagent (Invitrogen) and converted to complementary DNA by reverse transcriptase with AccuPower RocketScript RT premix (Bioneer). The quantitative real-time polymerase chain reaction reaction was performed with the FastStart Universal SYBR Green Master and Accupower 2×GreenStar Qpcr Master Mix (Bioneer). The relative expression level of mRNAs was normalized to β-actin mRNA as the internal control by using the $2^{-\Delta\Delta Ct}$ cycle threshold method. The forward and reverse primer sequences used to quantify ABCA1 and ABCG1 mRNA abundance were as follows: ABCA1 forward: AGATGCTTGGATAGGAGTGAGG, reverse: CTTCTTGGCTTCTGTATTGATGC; ABCG1 forward: AAGGATGAAGGCAGACGAGAG; reverse: TCAGAGACACCACTTGGAAGC.

Enzyme-Linked Immunosorbent Assay

The culture supernatants were collected after treatment of macrophages with or without exosomes (10 μg/mL) or lipopolysaccharide (500 ng/mL) as described for flow cytometry analysis. Then, the levels of IL-6 and tumor necrosis factor α were assessed with ELISA kits (NeoBioscience) according to the manufacturer's instructions, and the absorbance was measured using a Microplate Reader (Tecan Infinite M200).

Atherosclerotic Lesion Area Quantification

ApoE−/− mice were euthanized and the entire length of the aorta along with the heart was carefully exposed. For en face analysis, the aortas were cut longitudinally and stained with Sudan IV after removal of adventitia and AT. The images were captured with a Nikon D3000 digital camera (Nikon), and the extent of atherosclerotic lesions was analyzed using ImagePro Plus 6.0 software (Media Cybernetics). Cross-sectional analysis was performed to quantify atherosclerotic lesions at the aortic root. Briefly, the upper section of the heart with the aortic root was embedded in optimal cutting temperature compound and cryosectioned into 10-μm slices. The cross-sections were stained with Oil Red O and counterstained with hematoxylin. Images were captured with an optical microscope (DP73; Olympus) and the cross-sectional area of the atherosclerotic plaques was quantified using ImagePro Plus.

Immunofluorescence Staining of Aortic Sections

Aortic sections were cryosectioned in 10-μm intervals. After antigen retrieval and blocking with normal goat serum, the slices were incubated with primary antibodies against CD16/32 (ab25235; Abcam) and inducible nitric oxide synthase (ab178945; Abcam) overnight at 4° and then with appropriate fluorescence-conjugated secondary IgG antibodies (Beyotime Biotechnology) for 60 minutes in the dark at room temperature. 4',6-Diamidino-2-phenylindole was used to stain the cell nucleus. Fluorescence images were taken using a fluorescence microscope (BX53; Olympus). The CD16/32-positive area and inducible nitric oxide synthase–positive area were measured using ImagePro Plus.

In Vivo Macrophage Migration Assay

After administration with different kinds of AT-exosomes regularly, HFD-fed ApoE−/− mice were given 2 mL thioglycollate broth (3 g/100 mL) in subcutaneous injection. Three

days after the injection, mice were euthanized and peritoneal macrophages elicited from the mice were collected. Macrophagic cells from different groups were counted.

Statistical Analysis

All statistical analyses were performed with the statistical software SPSS package version 19.0 (IBM). Normal distribution of data was assessed with the Shapiro–Wilk test. If the data were normally distributed, statistical significance was evaluated with Student *t* test when only 2 value sets were compared or with 1-way ANOVA when the differences among groups were assessed (data presented as mean±SEM). For multiple comparisons, Dunnett multiple comparison test was applied. If the data failed normality tests, groups were compared using Wilcoxon rank-sum test for 2 groups and using Kruskal-Wallis test for more than 2 groups (data presented as median with 25th and 75th percentiles). Each experiment was repeated at least 3 times. A 2-tailed P value <0.05 was considered to be statistically significant.

Results

Characterization and Cellular Uptake of AT-Exosomes

As shown in Figure 1A, the exosomes derived from SAT and VAT of age-matched HFD-fed obese mice and WT lean mice were similar in size (20–100 nm) and had a cup-like shape, as shown by transmission electron microscopy. Quantitative analysis of exosomal protein levels showed that more exosomes were released in 12-hour ex vivo VAT cultures compared with SAT cultures. The quantity of exosomes in 12-hour ex vivo cultures of VAT from HFD-fed mice was significantly higher compared with that from age-matched lean mice (Figure 1B). The expression of exosomal identity markers TSG101, Alix, CD9, and heat shock protein cognate 70 was confirmed in exosomes released from the different groups of AT by Western blotting analysis (Figure 1C). We further determined whether AT-exosomes were effectively taken up by macrophages in vitro. Confluent Raw264.7 macrophages were cultured with PKH67-labeled (green) exosomes or the exosome-depleted fraction for 12 hours before imaging with a fluorescence microscopy. Green fluorescence was localized in the cytoplasm of macrophages, which was indicated by the red fluorescence of phalloidin, a well-established cytoskeletal stain, after PKH67-labeled exosome treatment (Figure 1D). The fluorescence staining did not differ among macrophages treated with the 4 groups of exosomes. The lack of green staining in the macrophages incubated with the exosome-depleted fraction excluded the possibility of PKH67 leakage. These data confirmed that AT-exosomes were successfully purified and could be effectively internalized by macrophages.

VAT Exosomes Enhance Macrophage Foam Cell Formation

Next, we examined the impact of AT-exosomes on the formation of macrophage-derived foam cells. Raw264.7 cells were cultured with oxLDL in the presence or absence of HFD-SAT exosomes, WT-SAT exosomes, HFD-VAT exosomes, or WT-VAT exosomes. Serum-free media was used in these experiments to exclude potentially confounding components in serum. Figure 2A through 2C summarizes the results of direct lipid analysis, which showed that HFD-VAT exosome-treated macrophages that were exposed to oxLDL accumulated ≈1.8-fold more total cholesterol, ≈1.6-fold more cholesterol esters, and ≈1.9-fold more free cholesterol than macrophages that were stimulated with oxLDL only (all $P<0.001$). Treatment with WT-VAT exosomes also markedly increased the total cholesterol, cholesterol ester, and free cholesterol content by ≈1.8-fold in oxLDL-stimulated macrophages (all $P<0.01$). However, HFD-SAT exosomes and WT-SAT exosomes did not alter the intracellular cholesterol accumulation induced by oxLDL. Furthermore, neutral lipid staining with Oil Red O revealed an obvious increase in oxLDL-mediated foam cell formation in macrophages exposed to either HFD-VAT exosomes or WT-VAT exosomes compared with macrophages that were maintained in exosome-free media (Figure 2D). Thus, exosomes released by VAT from both obese and lean mice, but not SAT exosomes, enhanced cholesterol accumulation and increased macrophage foam cell formation in vitro.

VAT Exosomes Prevent Cholesterol Efflux From Macrophages

To delineate the mechanism by which VAT exosomes accelerated the generation of cholesterol-engorged macrophage foam cells, we examined cholesterol uptake and efflux in macrophages cultured in HFD-SAT exosome-, WT-SAT exosome-, HFD-VAT exosome-, or WT-VAT exosome-supplemented media or exosome-free media. Fluorescence imaging showed that treatment with exosomes from different types of AT did not affect cholesterol uptake into Raw264.7 macrophages after 4 hours of exposure to DiI-oxLDL (Figure 3A). The mean fluorescence intensity was comparable among macrophages cultured with or without VAT-derived exosomes, as assessed by flow cytometry (Figure 3B). In contrast, treatment with HFD-VAT exosomes and WT-VAT exosomes markedly decreased NBD-cholesterol efflux to mature HDLs in lipid-laden Raw264.7 macrophages by ≈80% and 70%, respectively, when compared with controls (Figure 3C).

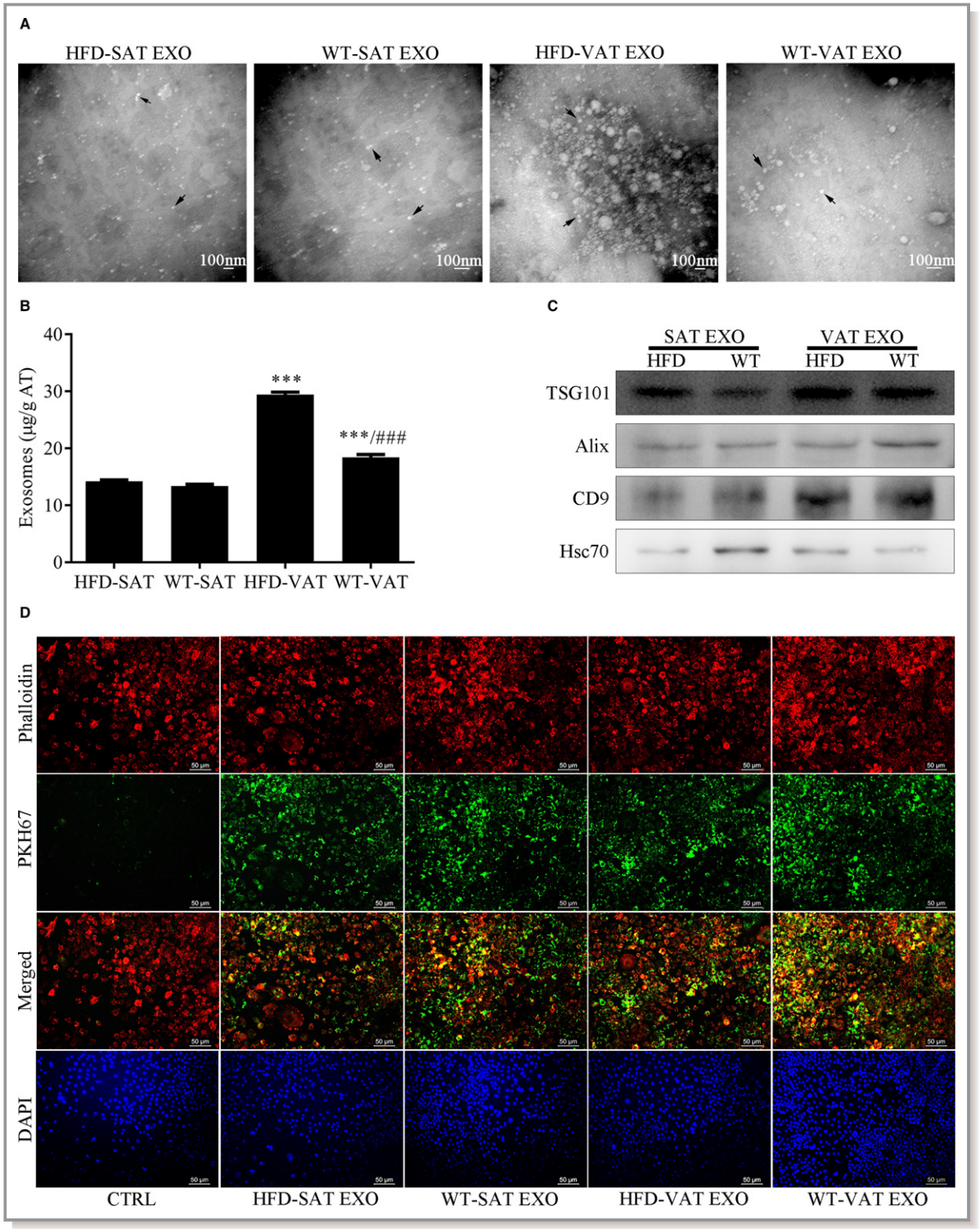

Figure 1. Characterization and cellular uptake of adipose tissue (AT)-exosomes (EXOs). A, AT-EXO characterization by transmission electron microscopy based on negative staining. Scale bars are annotated in each image. B, The amounts of EXO in the 12-hour ex vivo cultures of different types of AT explants (n=3 per group) were quantified using the bicinchoninc acid method, and the EXO level of per gram AT was presented as micrograms of total protein in EXOs (***P<0.001 vs high-fat diet [HFD]–subcutaneous AT [SAT], $^{\#\#\#}P$<0.001 vs HFD–visceral AT [VAT]). Data are presented as mean±SEM. C, Expression levels of the exosomal markers TSG101, Alix, CD9, and heat shock protein cognate 70 (Hsc70). D, Raw264.7 cells were incubated with PKH67 green membrane dye–labeled AT-EXOs or the EXO-depleted fraction (control group [CTRL]) for 12 hours and then fixed for fluorescence imaging (scale bar, 50 μm). Raw264.7 cells were also stained with phalloidin (red) and 4',6-diamidino-2-phenylindole (DAPI; blue). WT indicates wild-type mice.

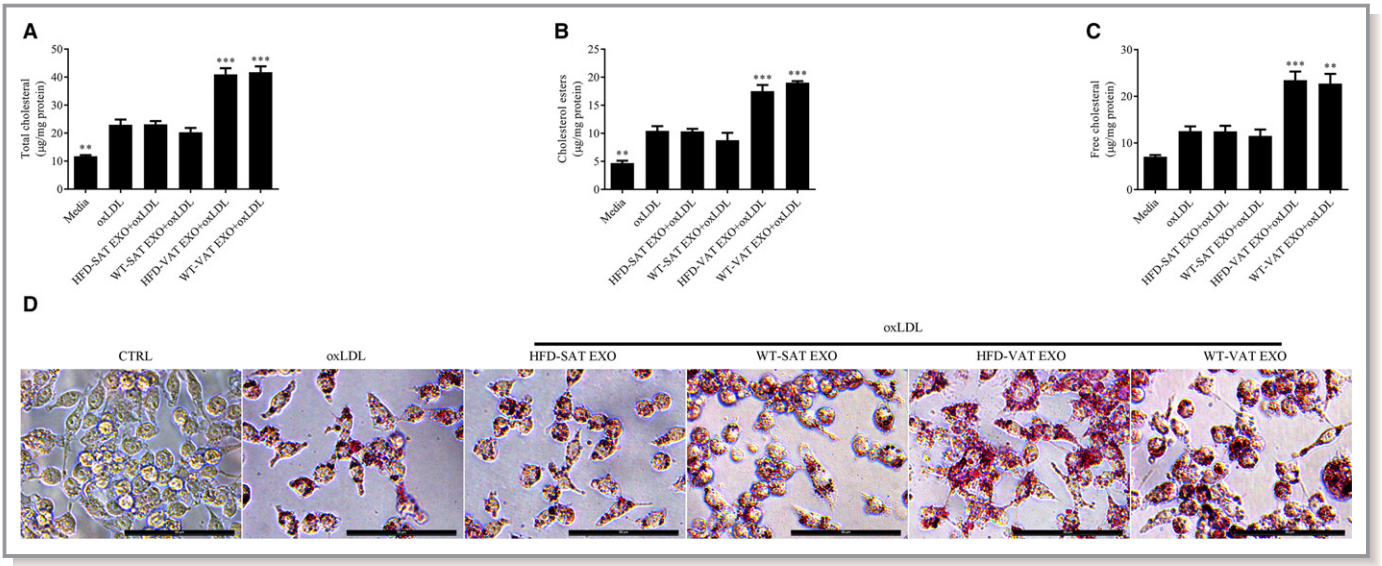

Figure 2. Visceral adipose tissue (VAT) exosomes (EXOs) enhance macrophage foam cell formation. A through C, Total cholesterol, cholesterol ester, and free cholesterol contents in Raw264.7 cells incubated with high-fat diet (HFD)–subcutaneous adipose tissue (SAT) EXO–, wild-type (WT)–SAT EXO–, HFD-VAT EXO–, or WT-VAT EXO–supplemented media or EXO-free media in the presence or absence of oxidized low-density lipoprotein (oxLDL) (***P<0.001 and **P<0.01 vs EXO-free oxLDL-treated cells). Data are presented as the mean±SEM of 3 independent experiments. D, Representative images of Oil Red O staining of cholesterol accumulation in Raw264.7 cells treated as described in Figure 2A through 2C (scale bar, 50 μm). CTRL indicates control group.

Similarly, NBD-cholesterol efflux caused by lipid-poor ApoA1 uptake was significantly attenuated by ≈80% in response to HFD-VAT exosome and WT-VAT exosome treatment (Figure 3D). However, HFD-SAT exosomes and WT-SAT exosomes did not produce notable effects on cholesterol efflux in Raw264.7 macrophages after 5 hours of stimulation with HDL or ApoA1 (Figure 3C and 3D). These data indicate clear differences between VAT- and SAT-derived exosomes in the regulation of macrophage cholesterol metabolism.

VAT Exosomes Dysregulate ABCA1, ABCG1, and LXR-α Expression in Macrophages

We then investigated the molecular mechanisms underlying the effect of AT-exosomes on cholesterol metabolism in macrophages by examining the expression level of lipid metabolism-related proteins. Raw264.7 macrophages were preincubated with different groups of AT-exosomes for 24 hours followed by cotreatment with or without 50 μg/mL oxLDL for another 6 hours. The protein expression levels are shown in Figure 4A and 4B. In accordance with the previously mentioned results, treatment with various groups of AT-exosomes did not alter the protein expression levels of CD36 and scavenger receptor A, critical membrane proteins that mediate cholesterol uptake, thus further excluding the possibility that VAT exosome–enhanced foam cell formation was attributed to an increase in lipid internalization. In addition, the protein expression of low-density lipoprotein receptor, a crucial target gene of SREBP2, was not influenced by AT-exosome treatment, implying that VAT exosome-induced intracellular lipid accumulation was not caused by increased endogenous lipid synthesis. ABCG1 and ABCA1 play important roles in cholesterol efflux during foam cell formation. Raw264.7 macrophages pretreated with HFD-VAT exosomes or WT-VAT exosomes expressed half the amount of ABCG1 and ABCA1 protein compared with control macrophages, which were only treated with oxLDL. Conversely, ABCG1 and ABCA1 protein expression was not notably changed by either HFD-SAT exosomes or WT-SAT exosomes. Polymerase chain reaction analysis of ABCA1 and ABCG1 mRNA expression revealed changes that were consistent with the changes in protein levels. Treatment with HFD-VAT exosomes or WT-VAT exosomes significantly decreased the mRNA levels of ABCA1 and ABCG1 in Raw264.7 macrophages (Figure 4C and 4D). Collectively, these results showed that VAT exosomes promoted macrophage foam cell formation by inhibiting the protein expression of transporters responsible for cholesterol efflux.

Because ABCA1 is regulated by the nuclear receptor LXR-α and ABCG1 is regulated by LXR-α as well as PPAR-γ, we next evaluated the protein level of LXR-α and PPAR-γ in oxLDL-treated macrophages (Figure 4A and 4B). LXR-α expression was markedly decreased in Raw264.7 macrophages cultured in HFD-VAT exosome– or WT-VAT exosome–supplemented media compared with macrophages stimulated with oxLDL only. In contrast, neither HFD-SAT exosomes nor WT-SAT exosomes exerted a significant influence on LXR-α protein expression. Moreover, none of the 4 AT-exosomes altered the

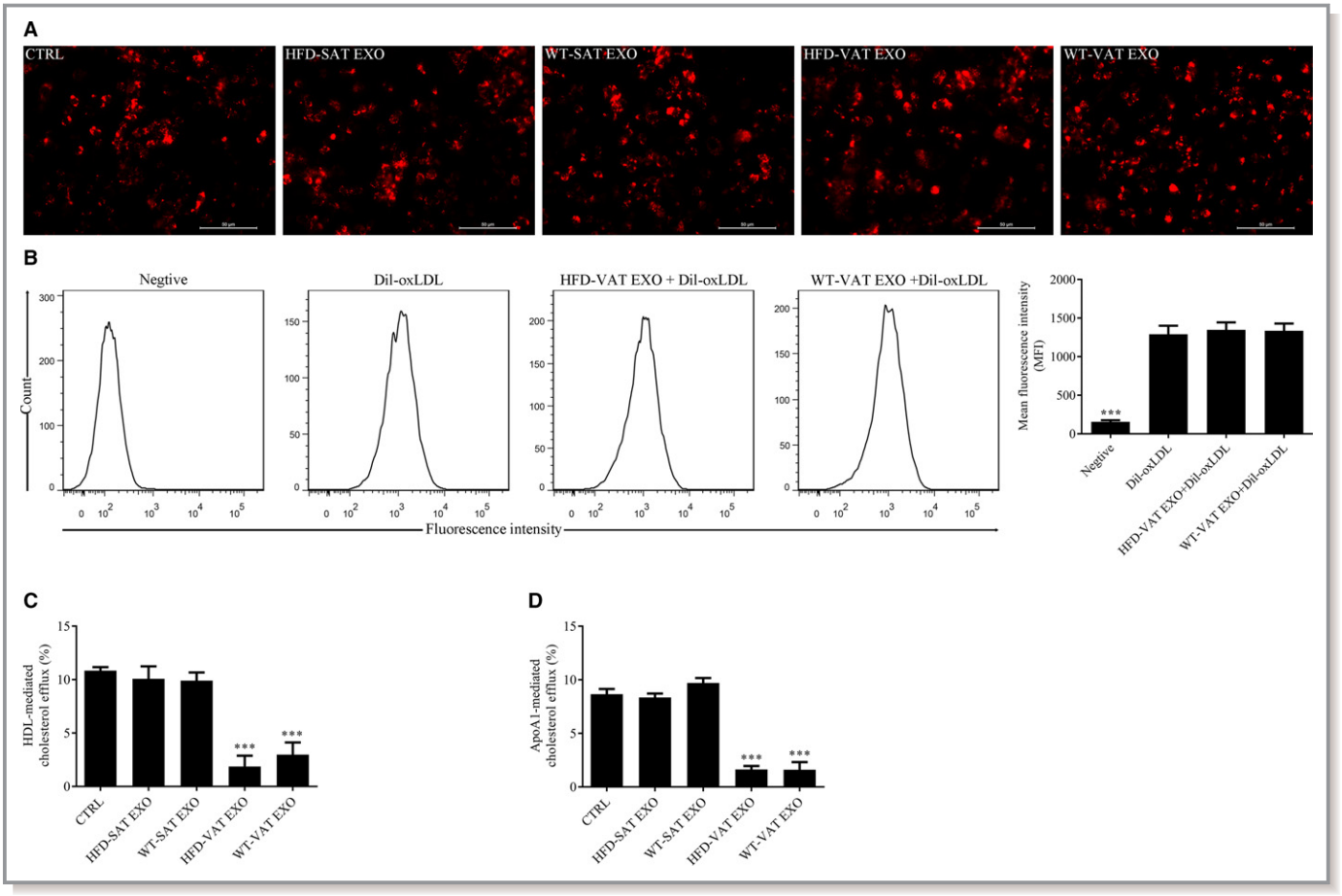

Figure 3. Visceral adipose tissue (VAT) exosomes (EXOs) prevent cholesterol efflux from macrophages. A, Cholesterol uptake, as determined by fluorescence microscopy in RAW264.7 macrophages pretreated with or without the different adipose tissue (AT)-EXOs. Red represents labeled-cholesterol uptake after 4 hours of exposure to Dil-oxidized low-density lipoprotein (Dil-oxLDL) (scale bar, 50 μm). B, Quantification of cholesterol uptake in Raw 264.7 cells cultured in VAT EXO-free and VAT EXO-supplemented media by assessing mean fluorescent intensity via flow cytometry analysis (***P<0.001 vs cells stimulated by Dil-oxLDL only). Representative images are shown. C and D, Raw264.7 cells loaded with nitrobenzoxadiazole (NBD)-labeled cholesterol were treated with AT-EXOs, and then cholesterol efflux to mature high-density lipoprotein cholesterol (HDL) (C) or lipid-free apolipoprotein A1 (apoA1) (D) was measured as indicated (***P<0.001 vs untreated cells). Data are presented as the mean±SEM of 3 separate experiments. CTRL indicates control group; HFD, high-fat diet–induced obese mice; SAT, subcutaneous adipose tissue; WT, wild-type mice.

protein expression level of PPAR-γ when cocultured with oxLDL, thus excluding the contribution of PPAR-γ to the effect of VAT exosomes. These data further suggest that the downregulation of LXR-α may be a common signaling pathway that mediates the decrease in ABCA1 and ABCG1 expression during VAT exosome–exacerbated macrophage foam cell formation.

HFD-VAT Exosomes Promote Macrophage Switching into the M1 Phenotype and NF-KB Activation

Since macrophages in atherosclerotic lesions are exposed to a myriad of M1- and M2-polarizing factors, we wondered whether AT-exosomes could affect the proinflammatory and anti-inflammatory potential of macrophages. Raw264.7 macrophages were incubated with various types of AT-exosomes or previously defined polarizing factors in serum-free medium for 24 hours to induce macrophage phenotype switching. Lipopolysaccharide and IL-4 stimulation were the positive controls for M1 and M2 polarization, respectively. As presented in Figure 5A and 5B, flow cytometry analysis showed that HFD-VAT exosome treatment significantly increased the proportion of M1 macrophages, as indicated by F4/80+/CD80+ cells. While 36.4% of the control macrophages exhibited the M1 phenotype, 61.6% of Raw264.7 macrophages polarized into the M1 phenotype upon exposure to HFD-VAT exosomes, which was slightly less than the lipopolysaccharide-stimulated macrophages, which exhibited 71.5% polarization into the M1 phenotype. The other 3 types of AT-exosomes did not exert a noticeable impact on M1 switching. With regard to M2 polarization, the addition of

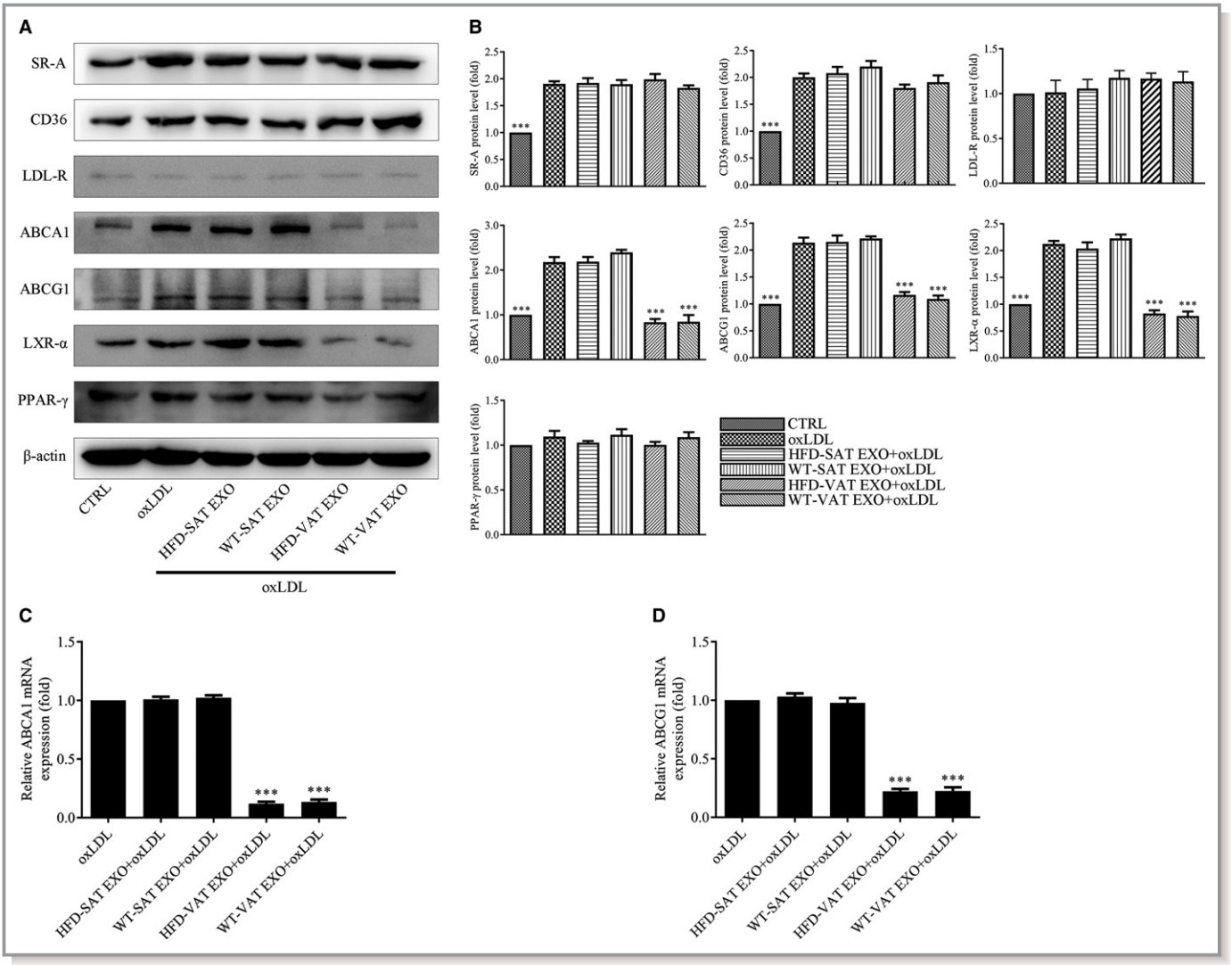

Figure 4. Visceral adipose tissue (VAT) exosomes (EXOs) dysregulate ABCA1, ABCG1, and liver X receptor α (LXR-α) expression in macrophages. Raw264.7 cells cultured in EXO-free or various adipose tissue (AT)-EXO–supplemented media were used to prepare total protein and RNA after treatment with oxidized low-density lipoprotein (oxLDL) for 6 hours. A, Western blotting analysis of scavenger receptor A (SR-A), CD36, low-density lipoprotein recptor (LDL-R), ABCA1, ABCG1, LXR-α, and peroxisome proliferator-activated receptor γ (PPAR-γ) expression. B, Quantification of protein expression levels normalized to β-actin. C, ABCA1 and (D) ABCG1 mRNA expression was determined by quantitative real-time polymerase chain reaction. Data are presented as the mean±SEM of 3 separate experiments. ***P<0.001 vs EXO-free oxLDL-stimulated cells. CTRL indicates control group; HFD, high-fat diet–induced obese mice; SAT, subcutaneous adipose tissue; WT, wild-type mice.

AT-exosomes had little effect on the ratio of F4/80+/CD206+ cells (Figure 5A through 5C). Thus, we focused on M1 polarization in the subsequent experiments. To further assess the influence of AT-exosomes on the production of the typical cytokines of M1 macrophages, we determined the concentration of tumor necrosis factor α and IL-6 in cell culture media using ELISA. Raw264.7 macrophages released ≈4-fold greater amounts of tumor necrosis factor α and ≈6-fold higher levels of IL-6 than control macrophages upon lipopolysaccharide stimulation. HFD-VAT exosome treatment significantly increased tumor necrosis factor α production in Raw264.7 macrophages by ≈3-fold (Figure 5D). In a parallel experiment, Raw264.7 macrophages treated by HFD-VAT exosomes released ≈3.5-fold higher amounts of IL-6 compared with the control group (Figure 5E). The exosomes from SAT and WT-VAT exosomes did not affect the production of the proinflammatory mediators. Because the transcription factor NF-κB plays a key role in M1 polarization by inducing the expression of various proinflammatory factors, we next evaluated its activity in Raw264.7 macrophages upon incubation with AT-exosomes. As shown by Western blotting analysis, HFD-VAT exosome treatment markedly induced the phosphorylation of NF-κB-p65 to an extent that was slightly inferior to that in the positive control without any change in total NF-κB-p65 expression (Figure 5F and 5G). However, the other 3 AT-exosomes did not affect the degree of NF-κB-p65

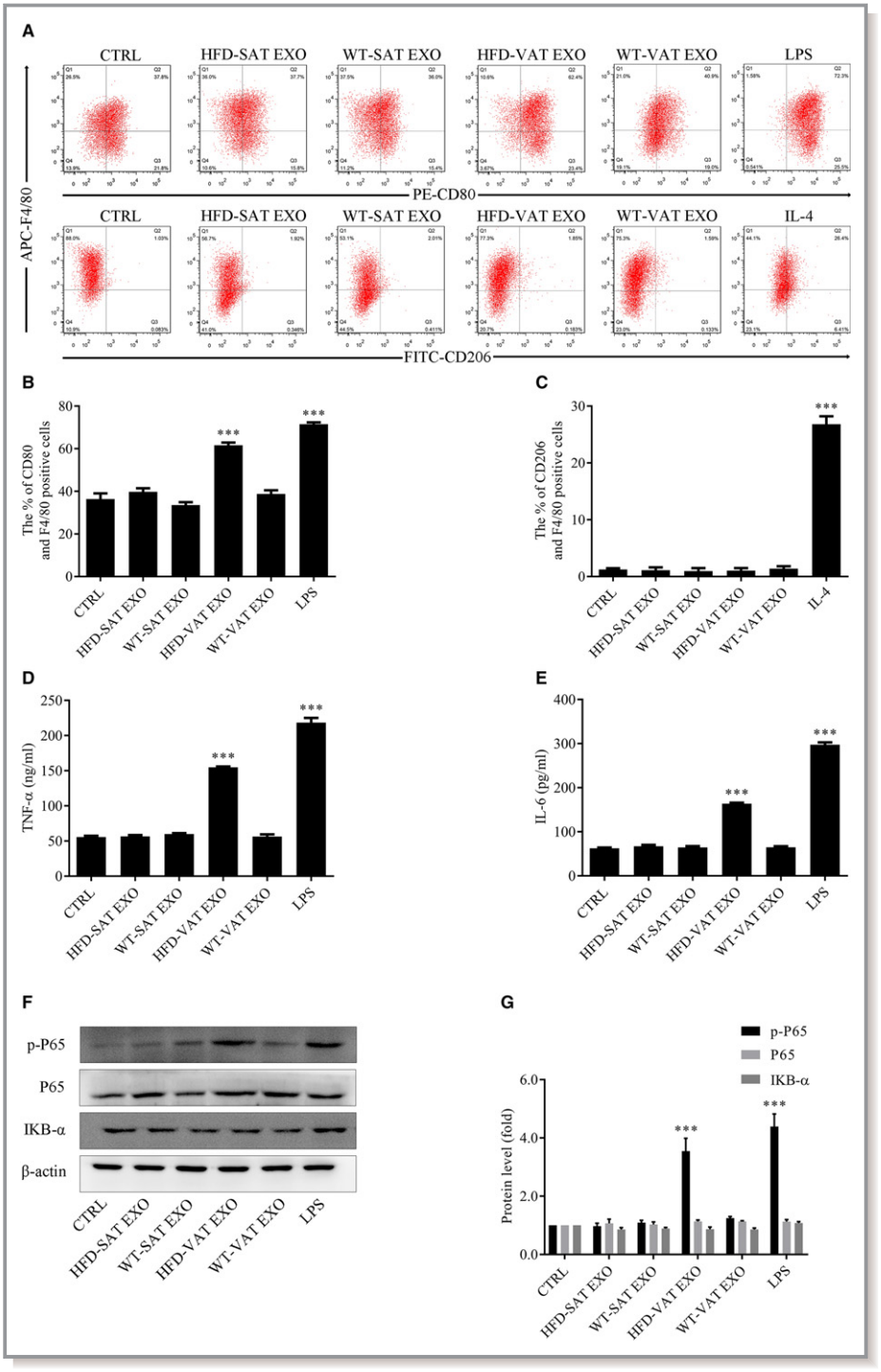

Figure 5. High-fat diet (HFD)–visceral adipose tissue (VAT) exosomes (EXOs) promote macrophage switching into the M1 phenotype and NF-KB activation. Raw264.7 cells were stimulated with or without different adipose tissue (AT)-EXOs, lipopolysaccharide (LPS), or interleukin (IL) 4 for 24 hours. A through C, The percentages of M1- and M2-polarized macrophages were separately analyzed by measuring CD80+/F4/80+ cells and CD206+/F4/80+ cells using flow cytometry, and the representative images of 3 independent experiments are shown. D and E, tumor necrosis factor α (TNF-α), and IL-6 levels in the supernatant were quantified by ELISA. F and G, Western blotting analysis of phospho-NF-κB-p65, total NF-κB-p65, and IκB-α expression; the protein expression levels are normalized to β-actin. Data are presented as the mean±SEM of 3 independent experiments. ***$P<0.001$ vs the nonstimulated group (CTRL). SAT indicates subcutaneous adipose tissue; WT wild-type mice.

phosphorylation. Moreover, the expression of IκB-α was identical in the presence or absence of different types of AT-exosomes (Figure 5F and 5G), excluding the possibility that this induction was accompanied by the degradation of IκB-α. Collectively, these data demonstrated that only HFD-VAT exosomes effectively promote M1 macrophage polarization, probably through the activation of NF-κB, but they did not have an obvious effect on M2 polarization.

Systemic Administration of HFD-VAT Exosomes Exacerbates Atherosclerosis in ApoE−/− Mice

To study the functional role of AT-exosomes in atherogenesis in vivo, we periodically administered AT-exosomes to ApoE−/− mice, which are mouse models of atherosclerosis. Fat deposition on total aortic surfaces and in aortic roots was assessed in these mice. Sudan IV staining of the whole aorta from mice injected with HFD-VAT exosomes showed significantly increased atherosclerotic lesion area compared with PBS-injected mice (Figure 6A and 6B). Moreover, Oil Red O–stained areas in cross-sections of the aortic sinus were profoundly increased in the HFD-VAT exosome–treated mice (Figure 6C and 6D). The administration of WT-VAT exosomes also tended to increase the area of lipid deposition, but the change was not statistically significant (Figure 6B through 6D). The lipid areas in aorta and plaque were of similar magnitude among the groups treated with SAT exosomes and PBS. Consistent with the results of in vitro experiment, HFD-VAT exosome treatment significantly decreased the protein expression of ABCA1 and ABCG1 in aortas of ApoE−/− mice (Figure 6E and 6F). Subsequently, the region of atherosclerotic lesions that was infiltrated by M1 macrophages was detected by a combined immunofluorescence staining using antibodies against CD16/32 and inducible nitric oxide synthase. The area stained with anti-M1 macrophage antibodies in the aortic roots from HFD-VAT exosome–injected mice was significantly increased compared with PBS-injected mice (Figure 7A and 7B). The corresponding area of mice treated with the other 3 types of AT-exosomes did not show a profound difference compared with the PBS-injected mice. However, the body weights and the plasma triglyceride and plasma cholesterol levels were similar among all groups (Figure 8A through 8E). Monocyte recruitment is another key determinant of the severity of atherosclerotic lesions. To test whether the administration of AT-exosomes affects macrophage recruitment in vivo, mice were intraperitoneally injected with thioglycollate. There were no differences in peritoneal macrophage counts among all groups (Figure 8F). Thus, the exosomes released by VAT from obese mice could promote atherogenesis in vivo without changes in plasma cholesterol levels and macrophage migration.

Discussion

In the present study, we demonstrated that visceral fat–derived exosomes, irrespective of obesity, facilitated macrophage-derived foam cell formation through the prevention of ABCA1- and ABCG1-mediated cholesterol efflux, probably in an LXR-α–dependent manner. We then found that only obese visceral fat–derived exosomes were capable of inducing M1 macrophage polarization by modulating NK-κB activity. The results of the in vivo studies further demonstrate that systematic administration of HFD-VAT exosomes leads to accelerated atherosclerosis in hyperlipidemic ApoE−/− mice. Taken together, this study provides novel evidence indicating the role of exosomes as an effective mediator between visceral fat tissue dysfunction and accelerated atherosclerosis with the potential to promote macrophage foam cell formation and M1 phenotype switching during atherogenesis.

In recent years, exosomes have emerged as important players in intercellular communication.[24] AT, as an active endocrine organ, has been shown to release abundant exosomes to exert its auto/paracrine and endocrine functions in addition to well-described adipokines.[25] Numerous studies have shown that adipose-derived exosomes are linked to diverse physiological and pathological processes, including lipid metabolism, obesity-related insulin resistance, angiogenesis, immunomodulation, and tumor development.[26] In addition, AT has recently been confirmed to constitute a major source of the exosomal miRNAs in circulation,[12] and therefore might make a particular contribution to the circulating exosome level. These findings led us to hypothesize that AT-exosomes were ideal soluble signals that could travel long distances in circulation and directly influx into atherosclerotic plaques through injured endothelium and intraplaque microvessles. Several previous studies have reported that exosomes that are released from hypertrophic adipocytes impair endothelial cell function, suggesting a possible role for exosomes in obesity-related atherosclerosis.[27,28] However, as macrophages are the best-studied contributors to atherosclerosis, we focused on the interaction between exosomes and macrophages. The present study is the first to show that dysfunctional VAT produces exosomes with proatherosclerotic properties that can regulate lipid deposition and inflammatory responses in macrophages, providing a novel mechanistic link between visceral obesity and atherosclerosis.

It is known that AT is a widely distributed and highly heterogeneous organ that is commonly classified as distinct subcutaneous and visceral fat. Abraham et al[29] prospectively demonstrated that VAT volume was more closely associated with the development of cardiovascular risk factors than SAT volume. VAT has been reported to predict the incidence of cardiovascular disease, such as hypertension and myocardial

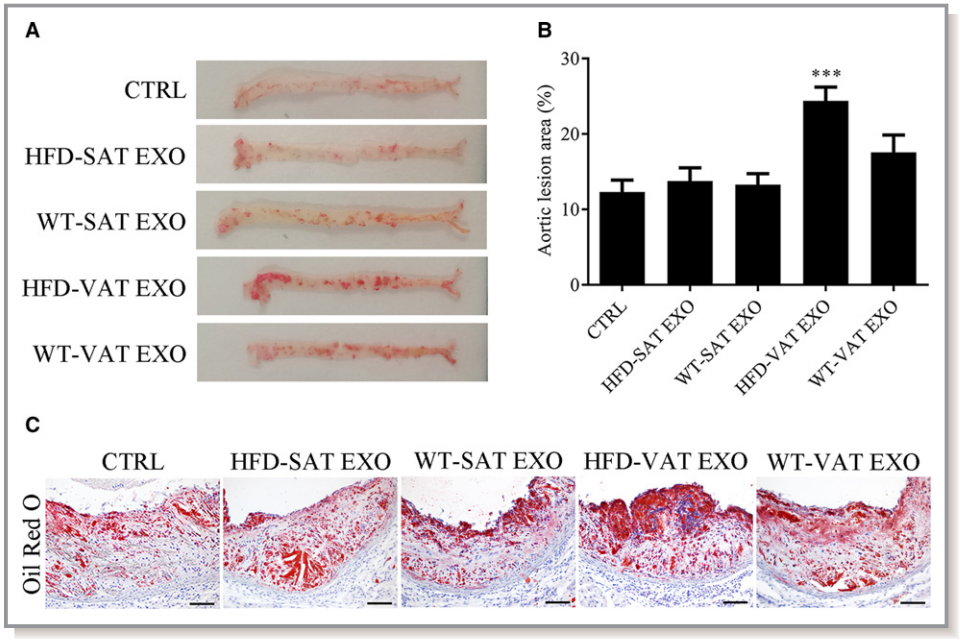

Figure 6. Systemic administration of high-fat diet (HFD)–visceral adipose tissue (VAT) exosomes (EXOs) exacerbates aortic lipid deposition in apolipoprotein E–deficient (ApoE−/−) mice. HFD-fed ApoE−/− mice were intravenously injected with different adipose tissue (AT)-EXOs or PBS periodically for 6 weeks. A, Representative images of en face Sudan IV staining of aortas from PBS (control group [CTRL])- or various adipose tissue (AT)-EXO (HFD–subcutaneous AT [SAT] EXOs, WT-SAT EXOs, HFD-VAT EXOs, or WT-VAT EXOs)–injected ApoE−/− mice. B, Quantification of the ratios of the Sudan IV–stained area to the aortic wall area in Figure 6A (n=6). C, Representative images of aortic root cross-sections that were stained with Oil Red O (scale bar, 100 μm). D, Quantification of the atheroma area stained by Oil Red O in Figure 6C (n=6). E, Representative Western blotting analysis of scavenger receptor A (SR-A), CD36, ABCA1, and ABCG1 expression from aortic lysates from mice injected with PBS and different AT-EXOs. F, Quantification of protein expression levels normalized to β-actin. Data are presented as mean±SEM. ***P<0.001, **P<0.01, *P<0.05 vs PBS-injected mice (CTRL). WT indicates wild-type mice.

infarction, among certain populations.[30–32] These evidences suggest that visceral fat is an ectopic depot that confers pathogenic risk beyond its contribution to overall obesity. Mechanically, visceral fat is more metabolically active than subcutaneous fat. It is characterized by a greater capacity to store and mobilize triglycerides, facilitating metabolic deterioration and atherosclerosis.[33] In addition, visceral fat but not subcutaneous fat has been reported to contain more macrophages, T lymphocytes, and mast cells in patients with coronary artery disease.[34,35] VAT produces a more proinflammatory cytokine profile and possesses a higher adipokine secretion ability than SAT.[6,36] Consistent with previous studies, we found that more exosomes were released by VAT compared with subcutaneous fat. Furthermore, we observed that the biological functions of AT-exosomes vary with the type of AT from which the exosomes are derived. VAT exosomes but not SAT exosomes are capable of enhancing macrophage foam cell formation, a key step in both early and late atherosclerotic lesions.

In addition to its heterogeneity, another key property of AT is its ability to change its metabolic status and functionality during the transition from the lean to the overweight state. Deng et al[37] found that exosomes from obese but not lean mouse VAT activated monocyte differentiation into macrophages and prompted insulin resistance. Exosomes from visceral fat of obese individuals may affect the development of nonalcoholic fatty liver disease.[38] miRNA profiles of VAT-derived exosomes from obese and lean individuals are different.[39] Presumably, obesity may cause dysregulation in the assembly of adipose-exosome biological components, resulting in the unregulated sorting of certain contents into exosomes. The results from the present study further show that VAT-derived exosomes from obese mice induced macrophage M1 phenotype transition by regulating NF-κB activity. Obesity is accompanied by chronic low-grade inflammation. It is conceivable that VAT exosomes, together with previously established proinflammatory cytokines and adipokines, constitute the inflammatory effectors of obese AT, exacerbating obesity-associated complications. Additionally, obesity always leads to relative hypoxia in AT caused by insufficient capillary network expansion. A previous study demonstrated that hypoxia profoundly increased exosome

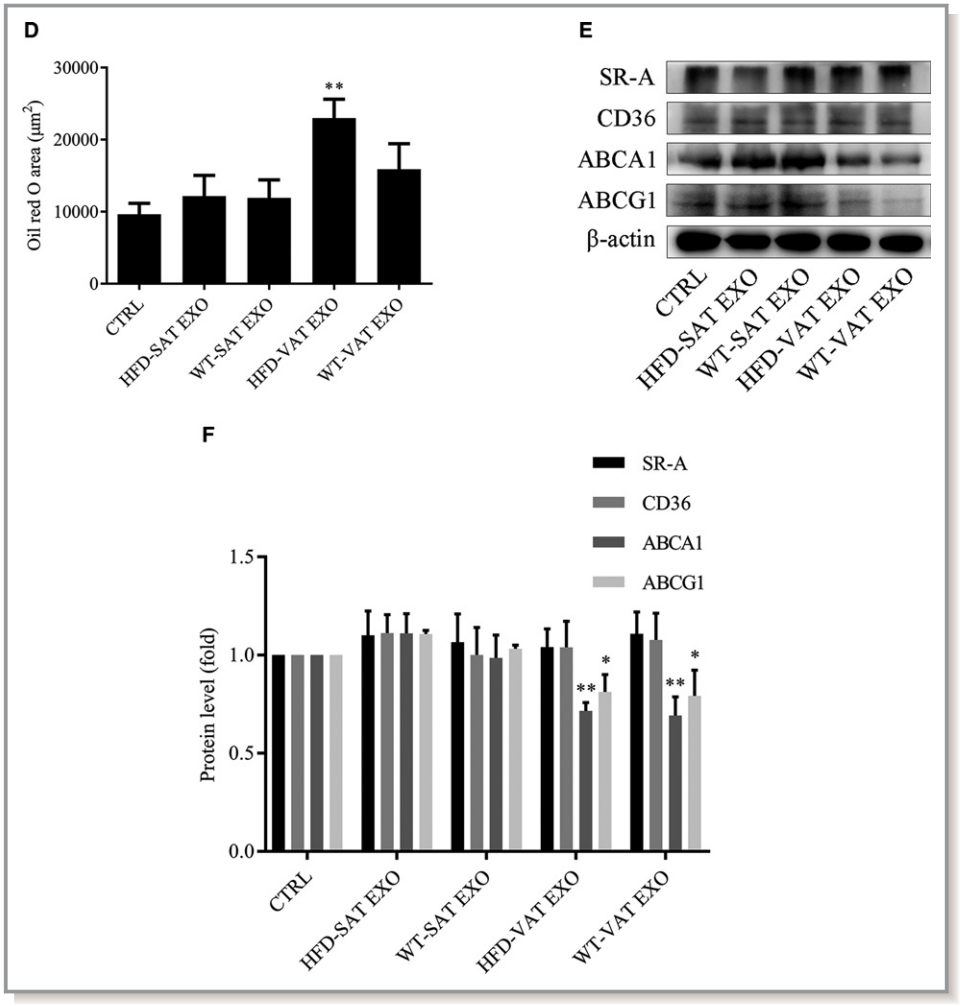

Figure 6. Continued

secretion by 3T3-L1 adipocyte and enhanced the volume of lipid droplets in adipocytes.[40] In line with the cited work, our findings show that VAT from obese mice secreted higher quantities of exosomes than VAT from lean VAT. However, the effect of fat-derived exosomes (the same amount) from obese and lean mice on macrophage foam cell formation was comparable. Nevertheless, we speculate that VAT from obese individuals has a more remarkable effect on macrophage foam cell formation, compared with an equal weight of VAT from lean individuals, in addition to the excess accumulation of visceral fat that occurs in obese individuals.

The formation of macrophage foam cells, which are characterized by the disruption of lipid homoeostasis in macrophages, is a vital feature of atherosclerosis.[41] Our results show that VAT exosomes treatment substantially enhanced the generation of macrophage-derived foam cells by reducing the expression of ABCA1 and ABCG1, key lipid transport proteins involved in mobilizing cholesterol out of macrophages and onto extracellular ApoA1 and HDL, respectively. Moreover, we found that the VAT exosome–induced upregulation of lipid accumulation in macrophages was accompanied by a decreased cellular level of LXR-α, which is a well-established nuclear receptor that mediates the transcription of ABCA1 and ABCG1. Collectively, these results suggest that VAT exosomes regulate a unifying cell signaling pathway that represses both ABC transporter expression and cholesterol efflux. However, the detailed molecular mechanisms merit further study. We also demonstrated that VAT-derived exosomes from obese individuals could aggravate inflammation by regulating the M1/M2 status of macrophages. The complex formed by NF-κB and IκB is a critical element in the regulation of this process.[42] As expected, HFD-VAT exosomes significantly increased the phosphorylation of NF-κB-p65 without influencing the levels of IκB-α, suggesting a possible mechanism by which HFD-VAT exosomes affect macrophage polarization. In addition, it was previously found that knockdown of ABCA1 in macrophages increased membrane cholesterol and lipid raft content, which promoted a toll-like receptor 4-MyD88–mediated proinflammatory response.[43] Therefore, the VAT exosome–induced

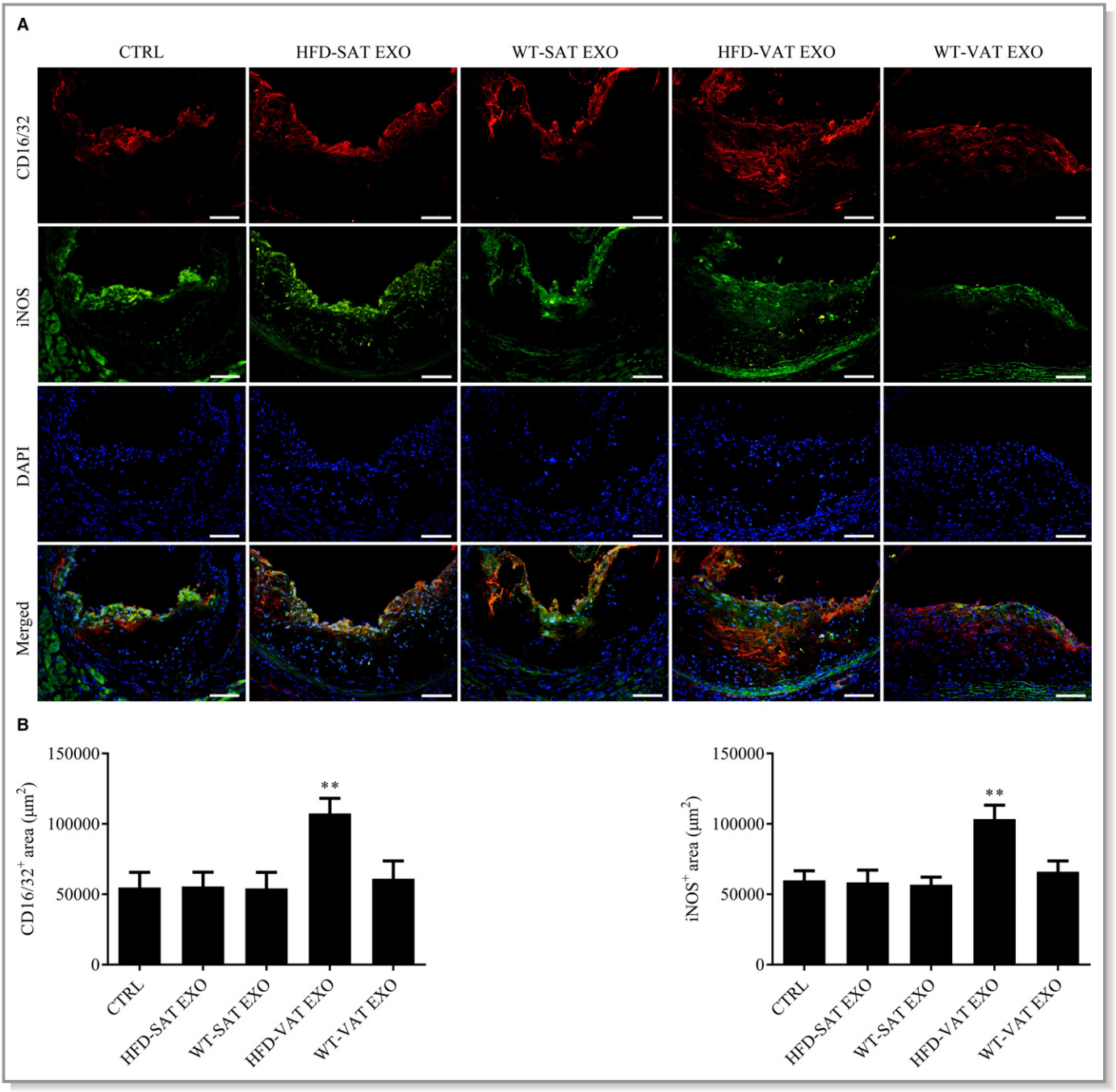

Figure 7. Systemic administration of high-fat diet–induced obese mice (HFD)–visceral adipose tissue (VAT) exosomes (EXOs) increases M1 macrophage proportion in atherosclerotic lesion of apolipoprotein E–deficient (ApoE−/−) mice. A, Atherosclerotic lesions in the aortic sinus from diverse adipose tissue (AT)–EXO- and PBS (control group [CTRL])-treated ApoE−/− mice were probed with specific antibodies against CD16/32 (red) and inducible nitric oxide synthase (iNOS) (green). The representative images are shown (scale bar, 100 μm). B, Quantification of the areas in the aortic sinus cross-sections stained for CD16/32 and iNOS (n=6). Data are presented as mean±SEM. $^{**}P<0.01$ vs PBS-injected mice (CTRL). DAPI indicates 4',6-diamidino-2-phenylindole; SAT, subcutaneous adipose tissue; WT, wild-type mice.

downregulation of cholesterol efflux in macrophages may also play a crucial role in regulating macrophage polarization and the inflammatory response. Given that the contents of exosomes are complex, the contribution of adipose-derived exosomes to certain biological events, such as macrophage foam cell formation and polarization, is likely multifactorial.

Finally, we intravenously injected AT-exosomes of diverse origins into experimental atherosclerosis mouse models, resulting in heterogeneous lesion severity and homogeneous whole-body metabolism, which provided direct evidence for the effect of exosomes from visceral fat of obese individuals on disease progression. In contrast to our results, Deng

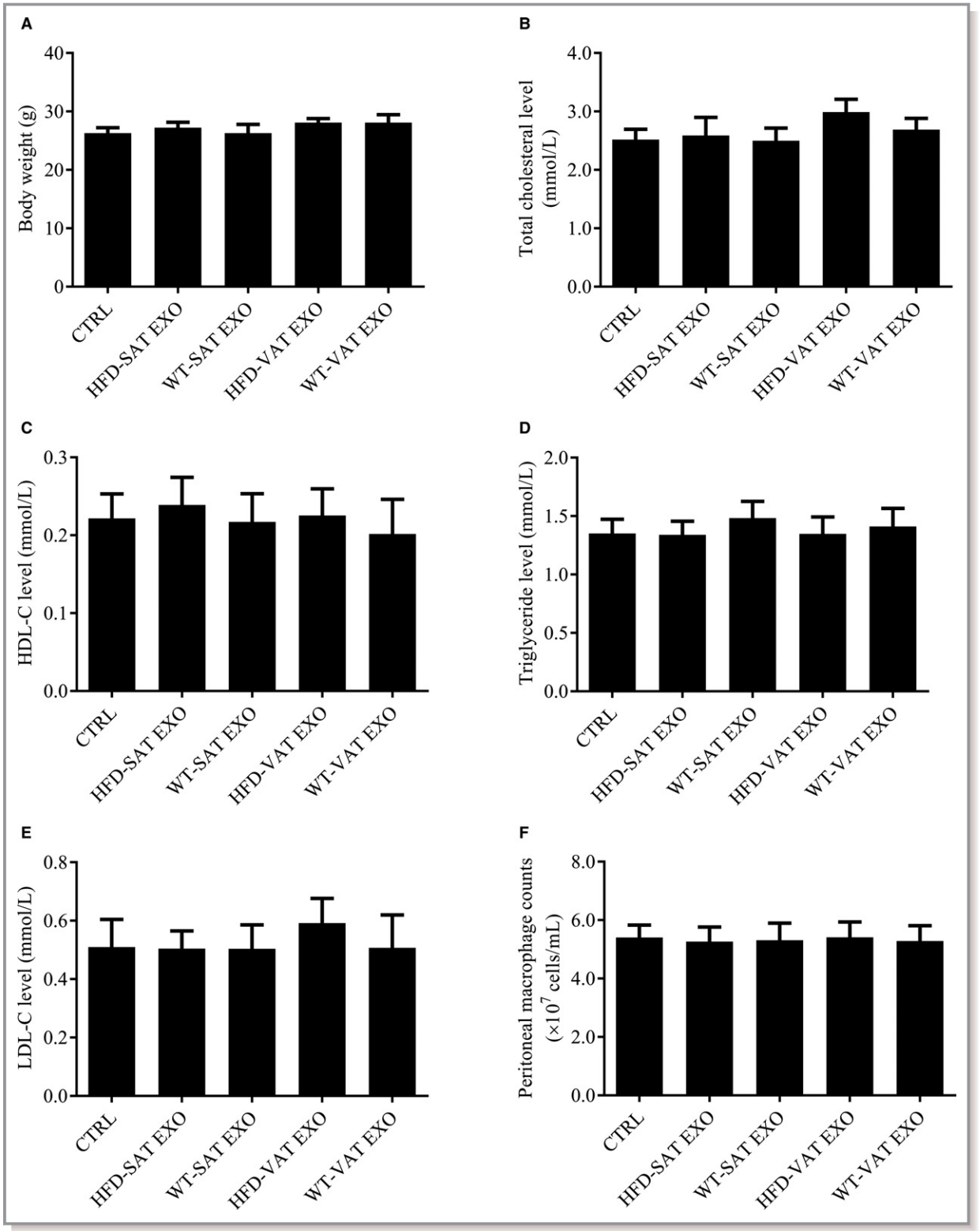

Figure 8. Administration of adipose tissue (AT)-exosomes (EXOs) does not affect body weight, lipid profile, and macrophage migration in apolipoprotein E–deficient (ApoE−/−) mice. High-fat diet (HFD)–fed obese ApoE−/− mice were injected with different AT-EXOs or PBS (control group [CTRL]) regularly for 6 weeks. A through E, Body weight, total cholesterol levels, triglycerides levels, and lipoprotein profiles were measured at the end of the procedure (n=6). F, Thioglycollate (3%w/v) was injected into the peritoneal cavity and after 3 days peritoneal macrophages were counted from different AT-EXO– or PBS-injected mice before euthanization (n=6). Data are presented as mean±SEM. HDL-C indicates high-density lipoprotein cholesterol; LDL-C, low-density lipoprotein cholesterol; SAT, subcutaneous adipose tissue; VAT, visceral adipose tissue; WT, wild-type mice.

et al[37] found that the administration of exosome-like vesicles from dysfunctional AT enhanced insulin resistance in WT mice, and therefore, those exosome-like vesicles may aggravate the lipid profile and adiposity. This discrepancy may be partly caused by the profound dyslipidemia and overweight status of all of our experimental HFD-fed ApoE−/− mice. The narrow range of plasma cholesterol levels and body weight may have limited the detection of differences in metabolic disturbance among groups. Moreover, the circulating adipokines such as adiponectin are closely associated with the progression of atherosclerosis,[44] and the lack of the serum levels of adipokines in the in vivo experiment may have limited the elimination of confounding factors. Nevertheless, the net effect of adipose-derived exosomes on the vascular wall is nonnegligible. In addition, though in vitro experiments demonstrated that both WT-VAT exosomes and HFD-VAT exosomes promoted macrophage foam cell formation, only HFD-VAT exosomes, which also induced M1 polarization in vitro, significantly increased lipid deposition in aorta in a mouse model. This may be explained by the complex interaction between inflammation and foam cell formation in plaque local environment, ie, macrophage cholesterol loading can slightly reduce the inflammatory response, whereas lipid accumulation in M1-polarized macrophages is profoundly augmented.[45,46] As such, our study adds a layer of complexity to the interpretation of the causal relationship between obesity and atherosclerosis, and provides a possible therapeutic target for arteriosclerotic cardiovascular disease in overweight individuals.

Conclusions

Our study shows that exosomes released from differently located and stressed ATs have distinct proatherosclerotic effects. Among them, VAT-derived exosomes from obese individuals were shown to play previously unknown pathophysiological roles both in macrophage foam cell formation and M1 macrophage polarization by downregulating ABCA1- and ABCG1-mediated cholesterol efflux and upregulating NF-κB activity, respectively, thereby accelerating atherosclerosis in vivo. The findings in this study reveal a novel mechanistic link between obesity and the progression of atherosclerosis and identify exosomes as a promising therapeutic target for the attenuation of atherosclerotic vascular disease in the growing obese population.

Sources of Funding

This study was supported by the National Natural Science Foundation of China (grant numbers 91739113, 81571749, 81330033, and 81703502).

Disclosures

None.

References

1. Van Gaal LF, Mertens IL, De Block CE. Mechanisms linking obesity with cardiovascular disease. *Nature*. 2006;444:875–880.
2. Kunimura A, Ishii H, Uetani T, Aoki T, Harada K, Hirayama K, Negishi Y, Shibata Y, Sumi T, Kawashima K, Tatami Y, Kawamiya T, Yamamoto D, Suzuki S, Amano T, Murohara T. Impact of nutritional assessment and body mass index on cardiovascular outcomes in patients with stable coronary artery disease. *Int J Cardiol*. 2017;230:653–658.
3. Kataoka Y, Hammadah M, Puri R, Duggal B, Uno K, Kapadia SR, Tuzcu EM, Nissen SE, Nicholls SJ. Plaque vulnerability at non-culprit lesions in obese patients with coronary artery disease: frequency-domain optical coherence tomography analysis. *Eur J Prev Cardiol*. 2015;22:1331–1339.
4. Yonetsu T, Kato K, Uemura S, Kim BK, Jang Y, Kang SJ, Park SJ, Lee S, Kim SJ, Jia H, Vergallo R, Abtahian F, Tian J, Hu S, Yeh RW, Sakhuja R, McNulty I, Lee H, Zhang S, Yu B, Kakuta T, Jang IK. Features of coronary plaque in patients with metabolic syndrome and diabetes mellitus assessed by 3-vessel optical coherence tomography. *Circ Cardiovasc Imaging*. 2013;6:665–673.
5. Kiliaan AJ, Arnoldussen IA, Gustafson DR. Adipokines: a link between obesity and dementia? *Lancet Neurol*. 2014;13:913–923.
6. Smekal A, Vaclavik J. Adipokines and cardiovascular disease: a comprehensive review. *Biomed Pap Med Fac Univ Palacky Olomouc Czech Repub*. 2017;161:31–40.
7. Schindler TH, Cardenas J, Prior JO, Facta AD, Kreissl MC, Zhang XL, Sayre J, Dahlbom M, Licinio J, Schelbert HR. Relationship between increasing body weight, insulin resistance, inflammation, adipocytokine leptin, and coronary circulatory function. *J Am Coll Cardiol*. 2006;47:1188–1195.
8. Robbins PD, Morelli AE. Regulation of immune responses by extracellular vesicles. *Nat Rev Immunol*. 2014;14:195–208.
9. Huber HJ, Holvoet P. Exosomes: emerging roles in communication between blood cells and vascular tissues during atherosclerosis. *Curr Opin Lipidol*. 2015;26:412–419.
10. Ogawa R, Tanaka C, Sato M, Nagasaki H, Sugimura K, Okumura K, Nakagawa Y, Aoki N. Adipocyte-derived microvesicles contain RNA that is transported into macrophages and might be secreted into blood circulation. *Biochem Biophys Res Commun*. 2010;398:723–729.
11. Zhang Y, Mei H, Chang X, Chen F, Zhu Y, Han X. Adipocyte-derived microvesicles from obese mice induce M1 macrophage phenotype through secreted miR-155. *J Mol Cell Biol*. 2016;8:505–517.
12. Thomou T, Mori MA, Dreyfuss JM, Konishi M, Sakaguchi M, Wolfrum C, Rao TN, Winnay JN, Garcia-Martin R, Grinspoon SK, Gorden P, Kahn CR. Adipose-derived circulating miRNAs regulate gene expression in other tissues. *Nature*. 2017;542:450–455.
13. Tamminen M, Mottino G, Qiao JH, Breslow JL, Frank JS. Ultrastructure of early lipid accumulation in ApoE-deficient mice. *Arterioscler Thromb Vasc Biol*. 1999;19:847–853.
14. Rajagopalan S, Meng XP, Ramasamy S, Harrison DG, Galis ZS. Reactive oxygen species produced by macrophage-derived foam cells regulate the activity of vascular matrix metalloproteinases in vitro. Implications for atherosclerotic plaque stability. *J Clin Invest*. 1996;98:2572–2579.
15. Aqel NM, Ball RY, Waldmann H, Mitchinson MJ. Monocytic origin of foam cells in human atherosclerotic plaques. *Atherosclerosis*. 1984;53:265–271.
16. Kunjathoor VV, Febbraio M, Podrez EA, Moore KJ, Andersson L, Koehn S, Rhee JS, Silverstein R, Hoff HF, Freeman MW. Scavenger receptors class A-I/II and CD36 are the principal receptors responsible for the uptake of modified low density lipoprotein leading to lipid loading in macrophages. *J Biol Chem*. 2002;277:49982–49988.
17. Westerterp M, Bochem AE, Yvan-Charvet L, Murphy AJ, Wang N, Tall AR. ATP-binding cassette transporters, atherosclerosis, and inflammation. *Circ Res*. 2014;114:157–170.
18. Tabas I, Bornfeldt KE. Macrophage phenotype and function in different stages of atherosclerosis. *Circ Res*. 2016;118:653–667.
19. Colin S, Chinetti-Gbaguidi G, Staels B. Macrophage phenotypes in atherosclerosis. *Immunol Rev*. 2014;262:153–166.
20. Xu R, Li C, Wu Y, Shen L, Ma J, Qian J, Ge J. Role of KCa3.1 channels in macrophage polarization and its relevance in atherosclerotic plaque instability. *Arterioscler Thromb Vasc Biol*. 2017;37:226–236.
21. Fang S, Xu Y, Zhang Y, Tian J, Li J, Li Z, He Z, Chai R, Liu F, Zhang T, Yang S, Pei C, Liu X, Lin P, Xu H, Yu B, Li H, Sun B. Irgm1 promotes M1 but not M2

macrophage polarization in atherosclerosis pathogenesis and development. *Atherosclerosis*. 2016;251:282–290.

22. McAlpine CS, Huang A, Emdin A, Banko NS, Beriault DR, Shi Y, Werstuck GH. Deletion of myeloid GSK3alpha attenuates atherosclerosis and promotes an M2 macrophage phenotype. *Arterioscler Thromb Vasc Biol*. 2015;35:1113–1122.
23. Wang X, Ding X, Nan L, Wang Y, Wang J, Yan Z, Zhang W, Sun J, Zhu W, Ni B, Dong S, Yu L. Investigation of the roles of exosomes in colorectal cancer liver metastasis. *Oncol Rep*. 2015;33:2445–2453.
24. Ridger VC, Boulanger CM, Angelillo-Scherrer A, Badimon L, Blanc-Brude O, Bochaton-Piallat ML, Boilard E, Buzas EI, Caporali A, Dignat-George F, Evans PC, Lacroix R, Lutgens E, Ketelhuth DF, Nieuwland R, Toti F, Tunon J, Weber C, Hoefer IE. Microvesicles in vascular homeostasis and diseases. Position Paper of the European Society of Cardiology (ESC) Working Group on Atherosclerosis and Vascular Biology. *Thromb Haemost*. 2017;117:1296–1316.
25. Villarroya J, Cereijo R, Villarroya F. An endocrine role for brown adipose tissue? *Am J Physiol Endocrinol Metab*. 2013;305:E567–E572.
26. Zhang Y, Yu M, Tian W. Physiological and pathological impact of exosomes of adipose tissue. *Cell Prolif*. 2016;49:3–13.
27. Muller G. Microvesicles/exosomes as potential novel biomarkers of metabolic diseases. *Diabetes Metab Syndr Obes*. 2012;5:247–282.
28. Kranendonk ME, de Kleijn DP, Kalkhoven E, Kanhai DA, Uiterwaal CS, van der Graaf Y, Pasterkamp G, Visseren FL; Group SS. Extracellular vesicle markers in relation to obesity and metabolic complications in patients with manifest cardiovascular disease. *Cardiovasc Diabetol*. 2014;13:37.
29. Abraham TM, Pedley A, Massaro JM, Hoffmann U, Fox CS. Association between visceral and subcutaneous adipose depots and incident cardiovascular disease risk factors. *Circulation*. 2015;132:1639–1647.
30. Kouli GM, Panagiotakos DB, Kyrou I, Georgousopoulou EN, Chrysohoou C, Tsigos C, Tousoulis D, Pitsavos C. Visceral adiposity index and 10-year cardiovascular disease incidence: the ATTICA study. *Nutr Metab Cardiovasc Dis*. 2017;27:881–889.
31. Gencer B, Auer R, de Rekeneire N, Butler J, Kalogeropoulos A, Bauer DC, Kritchevsky SB, Miljkovic I, Vittinghoff E, Harris T, Rodondi N. Association between resistin levels and cardiovascular disease events in older adults: the health, aging and body composition study. *Atherosclerosis*. 2016;245:181–186.
32. Figueroa AL, Takx RA, MacNabb MH, Abdelbaky A, Lavender ZR, Kaplan RS, Truong QA, Lo J, Ghoshhajra BB, Grinspoon SK, Hoffmann U, Tawakol A. Relationship between measures of adiposity, arterial inflammation, and subsequent cardiovascular events. *Circ Cardiovasc Imaging*. 2016;9:e004043.
33. Spalding KL, Bernard S, Naslund E, Salehpour M, Possnert G, Appelsved L, Fu KY, Alkass K, Druid H, Thorell A, Ryden M, Arner P. Impact of fat mass and distribution on lipid turnover in human adipose tissue. *Nat Commun*. 2017;8:15253.
34. Hirata Y, Tabata M, Kurobe H, Motoki T, Akaike M, Nishio C, Higashida M, Mikasa H, Nakaya Y, Takanashi S, Igarashi T, Kitagawa T, Sata M. Coronary atherosclerosis is associated with macrophage polarization in epicardial adipose tissue. *J Am Coll Cardiol*. 2011;58:248–255.
35. Yamada H, Sata M. Role of pericardial fat: the good, the bad and the ugly. *J Cardiol*. 2015;65:2–4.
36. Villaret A, Galitzky J, Decaunes P, Esteve D, Marques MA, Sengenes C, Chiotasso P, Tchkonia T, Lafontan M, Kirkland JL, Bouloumie A. Adipose tissue endothelial cells from obese human subjects: differences among depots in angiogenic, metabolic, and inflammatory gene expression and cellular senescence. *Diabetes*. 2010;59:2755–2763.
37. Deng ZB, Poliakov A, Hardy RW, Clements R, Liu C, Liu Y, Wang J, Xiang X, Zhang S, Zhuang X, Shah SV, Sun D, Michalek S, Grizzle WE, Garvey T, Mobley J, Zhang HG. Adipose tissue exosome-like vesicles mediate activation of macrophage-induced insulin resistance. *Diabetes*. 2009;58:2498–2505.
38. Koeck ES, Iordanskaia T, Sevilla S, Ferrante SC, Hubal MJ, Freishtat RJ, Nadler EP. Adipocyte exosomes induce transforming growth factor beta pathway dysregulation in hepatocytes: a novel paradigm for obesity-related liver disease. *J Surg Res*. 2014;192:268–275.
39. Ferrante SC, Nadler EP, Pillai DK, Hubal MJ, Wang Z, Wang JM, Gordish-Dressman H, Koeck E, Sevilla S, Wiles AA, Freishtat RJ. Adipocyte-derived exosomal miRNAs: a novel mechanism for obesity-related disease. *Pediatr Res*. 2015;77:447–454.
40. Sano S, Izumi Y, Yamaguchi T, Yamazaki T, Tanaka M, Shiota M, Osada-Oka M, Nakamura Y, Wei M, Wanibuchi H, Iwao H, Yoshiyama M. Lipid synthesis is promoted by hypoxic adipocyte-derived exosomes in 3T3-L1 cells. *Biochem Biophys Res Commun*. 2014;445:327–333.
41. Chistiakov DA, Bobryshev YV, Orekhov AN. Macrophage-mediated cholesterol handling in atherosclerosis. *J Cell Mol Med*. 2016;20:17–28.
42. Mattioli I, Sebald A, Bucher C, Charles RP, Nakano H, Doi T, Kracht M, Schmitz ML. Transient and selective NF-kappa B p65 serine 536 phosphorylation induced by T cell costimulation is mediated by I kappa B kinase beta and controls the kinetics of p65 nuclear import. *J Immunol*. 2004;172:6336–6344.
43. Zhu X, Owen JS, Wilson MD, Li H, Griffiths GL, Thomas MJ, Hiltbold EM, Fessler MB, Parks JS. Macrophage ABCA1 reduces MyD88-dependent Toll-like receptor trafficking to lipid rafts by reduction of lipid raft cholesterol. *J Lipid Res*. 2010;51:3196–3206.
44. Tian L, Luo N, Zhu X, Chung BH, Garvey WT, Fu Y. Adiponectin-AdipoR1/2-APPL1 signaling axis suppresses human foam cell formation: differential ability of AdipoR1 and AdipoR2 to regulate inflammatory cytokine responses. *Atherosclerosis*. 2012;221:66–75.
45. Wolfs IM, Donners MM, de Winther MP. Differentiation factors and cytokines in the atherosclerotic plaque micro-environment as a trigger for macrophage polarisation. *Thromb Haemost*. 2011;106:763–771.
46. da Silva RF, Lappalainen J, Lee-Rueckert M, Kovanen PT. Conversion of human M-CSF macrophages into foam cells reduces their proinflammatory responses to classical M1-polarizing activation. *Atherosclerosis*. 2016;248:170–178.